

Bathymetric data coverage and density from single-beam and multibeam echo sounding surveys using unmanned surface vehicles in shallow inland waters

Oktawia Specht 

Gdynia Maritime University, Department of Transport, Morska St, 81–87, 81-225 Gdynia, Poland

RECEIVED 04.09.2025

ACCEPTED 30.10.2025

AVAILABLE ONLINE 16.02.2026

Abstract: Hydrographic surveys must comply with the IHO S-44 standard. For the most stringent orders (Exclusive, Special, and 1a), 100% seafloor coverage is required, posing challenges in shallow waters near the 1 m isobath. Recent advancements in unmanned surface vehicles (USVs) and the miniaturisation of hydroacoustic devices now enable high-precision surveys even in hard-to-access areas. This study presents an analysis of bathymetric data coverage and density obtained using singlebeam echosounders (SBES) and multibeam echosounders (MBES) systems mounted on unmanned surface vehicle (USVs). The SBES survey employed the AutoDron USV, while MBES data were collected with the HydroDron-1 USV. Coverage analysis used a 1×1 m grid. The results reveal significant differences between the two systems. The MBES achieved an average density of 7.71 pts·m⁻² (>94% of grid cells meeting the NOAA-recommended minimum of 5 pts·m⁻²). Data of MBES also exhibited uniform coverage, supporting the development of high-resolution bathymetric models. By contrast, SBES produced an average density of only 0.69 pts·m⁻², with a sparse and irregular point distribution. Only 1.79% of grid cells met the recommended threshold, while 63.79% contained no data. Nevertheless, SBES proved effective in the very shallow nearshore zone inaccessible to MBES. To achieve full coverage in compliance with International Hydrographic Organization's requirements, complementary methods such as bathymetric light detection and ranging, Global Navigation Satellite Systems-real time kinematic surveys, or structure from motion photogrammetry are essential. Integrating these technologies is required to produce reliable and complete seafloor models.

Keywords: bathymetric data, data coverage; data density, multibeam echosounders (MBES), singlebeam echosounders (SBES), unmanned surface vehicle (USV)

INTRODUCTION

Bathymetric data form a crucial foundation for numerous analyses conducted in aquatic environments, serving both scientific and practical purposes. They are used in navigation (Gao, 2009), flood risk management (Fernández-Nóvoa, González-Cao and García-Feal, 2024), shoreline erosion monitoring (David *et al.*, 2021), water engineering (Lubczonek *et al.*, 2022), environmental protection (Bentivoglio *et al.*, 2022), and geospatial analyses supported by Geographic Information Systems (GIS) (Gao, 2009).

Accurate mapping of seabed topography is becoming increasingly important due to the growing scale of hydrotechnical projects, the expansion of water infrastructure, and the need to monitor environmental changes in aquatic ecosystems. Particu-

larly challenging yet essential areas of research include coastal and shallow water zones, where bathymetric measurements are technically demanding and dynamic morphological processes frequently occur (Makar, 2023).

The development of measurement technologies in recent decades has led to the widespread use of hydroacoustic bathymetric systems (Lubis *et al.*, 2019). Among these, single-beam echosounders (SBES) and multibeam echosounders (MBES) are the most widely used and significant. These two types of systems differ in their operational characteristics, measurement accuracy, spatial resolution, and overall efficiency, all of which depend on environmental conditions and the depth of the surveyed waterbody (Khomsin, Pratomo and Saputro, 2021).

An SBES is a hydroacoustic device used to measure the distance, and thus the depth, between the transducer and the seabed or objects located in the water column. It is equipped with a transducer that emits a single acoustic beam directed vertically downward (Purnawan *et al.*, 2025). To function properly, a bathymetric system based on SBES must also include a positioning system, typically a Global Navigation Satellite System (GNSS)-real-time kinematic (RTK) receiver (Specht, Specht and Dabrowski, 2017). The footprint depends on the parameters of the echo sounder. It takes the shape of an acoustic cone, with the beamwidth corresponding to the opening angle in the plane perpendicular to the vessel's direction of movement (IHO, 2005).

In scientific applications, echo sounders with a narrow beam (up to 10°) are most commonly used, as they offer high vertical and angular resolution but limit the width of the coverage area (Salamon, 2006). Singlebeam echosounders are employed in various fields, including as navigational devices for observing the seabed and detecting underwater obstacles (Popielarczyk, 2011), as hydrographic tools for visualising seabed topography and structure (Haris *et al.*, 2012; Arseni *et al.*, 2019), and as fish-finding instruments for locating schools of fish (Landero Figueroa *et al.*, 2021). Due to their compact size and ease of use, SBES are also widely used in coastal zone monitoring, particularly in shallow water areas (Li *et al.*, 2023; Makar, 2023).

An MBES is an advanced hydroacoustic device designed to measure the depth between the transducer and the seabed or other objects located in the water column. Unlike SBES, an MBES emits multiple acoustic beams simultaneously at various angles relative to the vertical axis, creating a swath that enables data collection across the entire width of the survey strip (Mitchell and Hughes Clarke, 1994). These devices are equipped with two sets of transducers (transmitting and receiving), as well as additional components such as a motion reference unit (MRU), an inertial navigation system (INS), a sound velocity sensor (SVS), and a high-precision GNSS RTK positioning system (Stateczny, Groncka-Sledz and Motyl, 2019). Some modern MBES models are capable of generating up to 1,024 beams within a sector of 210°, enabling very high measurement density and full seabed coverage (Grządziel, 2022; NORBIT, 2022).

The MBES currently dominate depth measurement techniques and are used in both shallow and deep-water environments (Gao, 2009). They enable simultaneous measurements at hundreds of points, making them highly effective for identifying geotechnical obstacles, detecting gas leaks from the seabed (Orange *et al.*, 2002), classifying seafloor structures and sediments (Todd *et al.*, 1999), imaging benthic habitats (Trzcinska *et al.*, 2020), mapping navigational hazards, and planning cable and pipeline routes (Jung *et al.*, 2002). This technology is particularly effective at depths greater than 2 m, where the use of SBES is often limited by reduced range or lower resolution. Due to their very high measurement density, which can locally reach several dozen points per square meter in the nadir area, MBES systems have become the standard tool in modern marine and inland hydrography (Mohammadirojdan *et al.*, 2025).

Traditional bathymetric measurements conducted using an echo sounder from a manned hydrographic vessel are inefficient in shallow and hard-to-reach waterbodies due to the risk of equipment damage, low data resolution, high time demands, and difficulties in mapping the transitional zone near the 1-meter

isobath (Gao, 2009). To overcome these limitations, USVs equipped with miniature hydroacoustic devices are increasingly being employed (Specht, 2023). These systems enable the acquisition of high-resolution, high-precision bathymetric data, allowing for accurate mapping of seabed topography in shallow coastal areas. The following section presents a review of the literature on the density of bathymetric data collected using hydroacoustic devices mounted on both manned and unmanned measurement platforms.

Li *et al.* (2023) provide a comprehensive overview of current bathymetric data acquisition methods and their impact on measurement accuracy and spatial density. They discuss techniques such as SBES, MBES, airborne lidar bathymetry (ALB), structure from motion (SfM) photogrammetry, and satellite-derived bathymetry (SDB). The authors note that SBES yields very low data density, as measurements are taken only along individual survey lines, requiring extensive spatial interpolation and resulting in discontinuous seafloor coverage. In contrast, MBES allows for complete seafloor coverage, with data densities reaching up to $100 \text{ pts}\cdot\text{m}^{-2}$. The ALB typically achieves between 5 and $15 \text{ pts}\cdot\text{m}^{-2}$, while SfM can deliver up to $400 \text{ pts}\cdot\text{m}^{-2}$, although its application is limited to coastal zones. The SDB provides the lowest density, often below $1 \text{ pts}\cdot\text{m}^{-2}$, and its accuracy depends heavily on optical water conditions. The choice of method depends on environmental characteristics, equipment availability, required precision, and project budget. The SBES is most suitable for small-scale, low-cost projects, MBES is widely regarded as the standard in marine hydrography, and ALB and SfM are particularly effective for rapid data collection in shallow or hard-to-access coastal areas.

The "Hydrographic survey specifications and deliverables" report (Office of Coast Survey, 2021) outlines the standards and requirements for bathymetric measurements. As a part of project H13471, surveys were carried out using a Reson SeaBat 7125 MBES (400 kHz) mounted on the research vessel R/V Ocean Explorer. The measurement system operated in conjunction with a geodetic GNSS receiver, a MRU, a SVS, and CARIS Hydrographic Information Processing System / Sonar Imagery Processing System (HIPS/SIPS) software. The objective was to achieve complete and accurate seafloor coverage. According to the report's guidelines, a minimum density of five soundings per $1\times 1 \text{ m}$ grid cell is required. During the survey, a significantly higher data density was achieved. In many areas, particularly in the nadir region (the central part of the MBES beam), the density reached up to $20 \text{ pts}\cdot\text{m}^{-2}$. The data underwent comprehensive quality control, and invalid measurements such as multipath returns and acoustic noise were filtered out. The final bathymetric model met all accuracy and coverage criteria in accordance with the standards for International Hydrographic Organization (IHO) Order 1a.

Mohammadirojdan *et al.* (2025) present an advanced method for improving the quality of digital bathymetric models (DBMs) through the integration of measurement uncertainty analysis. The authors developed a comprehensive uncertainty model for hydrographic systems based on the principles of the Guide to the expression of uncertainty in measurement (GUM) and the Monte Carlo method. The model accounts for system-related, environmental, and geometric factors. To validate the approach, a measurement simulator was designed to generate MBES data over a synthetic seabed surface with known geometry.

Field studies were conducted in the Kiel Canal, at depths of up to 13 m, using the research vessel Uwe Jens Lornsen and a dual-head Kongsberg EM2040C MBES. Very high data density was achieved, with up to 45 pts·m⁻² in the nadir region and approximately 15 pts·m⁻² at the edges of the swath. The distance between successive pings along the survey line was approximately 0.35 m, while the point spacing across the track ranged from 0.06 to 0.4 m. Monte Carlo simulations demonstrated that incorporating uncertainty as weights in the surface modelling process using the multilevel B-spline approximation (MBA) method significantly improves the precision and stability of the resulting DBM, especially in the vertical dimension. The study confirms that integrating measurement uncertainty with high spatial data density and resolution is essential for producing reliable bathymetric models.

Lubczonek *et al.* (2022) present a method for generating continuous bathymetric models in shallow and very shallow waters by integrating data collected from unmanned measurement platforms, both aerial and surface-based. Measurements using a USV were conducted with an SBES along parallel survey lines spaced 10 meters apart. Measurement points were recorded every 30–40 cm along each profile. Based on these data, the approximate measurement density was estimated at 0.29 pts·m⁻². The USV data were characterised by stability, high precision, and the absence of local disturbances. In comparison, data obtained from UAVs using photogrammetric methods exhibited irregular but significantly higher point densities, ranging from 1 to over 300 pts·m⁻², depending on depth and optical conditions. Point density decreased with increasing depth, and the UAV point cloud showed greater vertical variability, caused in part by the presence of underwater vegetation and inaccuracies in photogrammetric reconstruction. The authors used a reference surface generated from the USV data to select reliable points from the UAV point cloud. This enabled the integration of both datasets into a single continuous bottom model. The proposed method supports detailed terrain representation from the shoreline to the deeper parts of the waterbody and is applicable in hydrographic mapping, habitat protection, and environmental monitoring.

Modern bathymetry requires not only high depth measurement accuracy but also sufficient seafloor coverage, particularly in the context of the IHO S-44 standard (IHO, 2022). Meeting the requirements for the Exclusive Order, Special Order, and Order 1a involves achieving 100% bathymetric coverage, which is especially challenging in shallow water zones, particularly near the 1-metre isobath. However, the development of USVs and the miniaturisation of hydroacoustic equipment now enable precise bathymetric measurements even in shallow and hard-to-access waterbodies.

The literature extensively discusses the accuracy of measurements obtained using various systems, including SBES, MBES, optical methods (SfM and ALB), and SDB. Nonetheless, there remains a lack of studies that comprehensively analyse the spatial density and coverage of bathymetric data acquired using SBES and MBES, particularly in shallow water environments.

This article presents a comparative analysis of bathymetric data acquired using SBES and MBES echo sounders mounted on USV platforms in shallow inland waters, with a focus on point cloud density, spatial resolution, and coverage uniformity with respect to the characteristics of each hydroacoustic system.

MATERIALS AND METHODS

CHARACTERISTICS OF SINGLEBEAM ECHOSOUNDERS DATA

Depth data obtained using an SBES are limited to a small area directly beneath the transducer. This limitation arises from the operating principle of the SBES, which records depth along a single, vertical acoustic beam. Consequently, these data do not meet the minimum bathymetric coverage requirements for the IHO orders: Exclusive, Special, and 1a, which require at least 100% coverage of the seabed topography. However, SBES measurements comply with the requirements for Orders 1b and 2, where only 5% coverage is permitted, and the maximum distance between adjacent survey lines is specified as no greater than three to four times the water depth (IHO, 2022). Some international standards specify a maximum spacing between profiles of 10 m.

The SBES generates point data along profiles, resulting in linear and discontinuous datasets. A typical measurement includes depth (d_e), coordinates (X, Y) from a GNSS receiver, and a timestamp (t). Depending on the system configuration, additional attributes such as signal quality, echo amplitude, or data from an inertial measurement unit (IMU) may also be recorded. Sampling frequency and acoustic beamwidth directly affect the spatial density of measurement points, which is critical for constructing accurate bathymetric models (Apollo *et al.*, 2024).

The limited spatial range of data necessitates conducting measurements along a greater number of profiles, which significantly increases the time required for bathymetric data acquisition (Bodus-Olkowska and Włodarczyk-Sielicka, 2013). To reduce the risk of missing seabed features, surveys are often supplemented with additional sonar passes between profiles, ensuring more complete seabed coverage. Due to the low spatial density of data, seabed surface models are generated using spatial interpolation. The choice of interpolation method (e.g., inverse distance weighting (IDW), kriging, splines) influences the quality of the model and the level of uncertainty, especially in areas with complex seabed topography (Arseni *et al.*, 2019).

Despite limited spatial coverage, measurements performed using an SBES can satisfy the accuracy requirements specified for the relevant IHO orders (IHO, 2022; Tuno *et al.*, 2024). Achieving this depends on proper system calibration, correction of systematic errors, and the application of appropriate data processing procedures. With carefully planned data acquisition and analysis, SBES can serve as a reliable tool even in more demanding applications.

In the context of using an SBES on USV platforms, stabilisation of the measurement platform and precise navigation of the vessel along planned survey lines are especially important. Due to their low displacement and lightweight construction, USVs are more susceptible to wave motion, which affects course stability and the quality of depth data. To minimise measurement errors, survey routes should be carefully designed, taking into account current hydrometeorological conditions (Specht *et al.*, 2020).

CHARACTERISTICS OF MULTIBEAM ECHOSOUNDERS DATA

Unlike SBES, MBES systems enable the simultaneous recording of multiple acoustic beams, thereby providing complete coverage of the seabed surface. As a result, bathymetric measurements conducted with MBES meet the accuracy requirements specified for the most stringent IHO orders: Exclusive, Special, and 1a.

These categories require at least 100% coverage of the seabed surface (IHO, 2022). Consequently, there is no need to perform additional measurements between survey lines.

The difference in seabed coverage between measurements recorded using an SBES and those recorded with an MBES is illustrated in Figure 1. While SBES performs point measurements along profiles, resulting in large gaps between data points and limited spatial information, MBES offers dense and continuous coverage of the entire seabed surface within the swath, significantly enhancing obstacle detection and the accuracy of seabed topography representation.

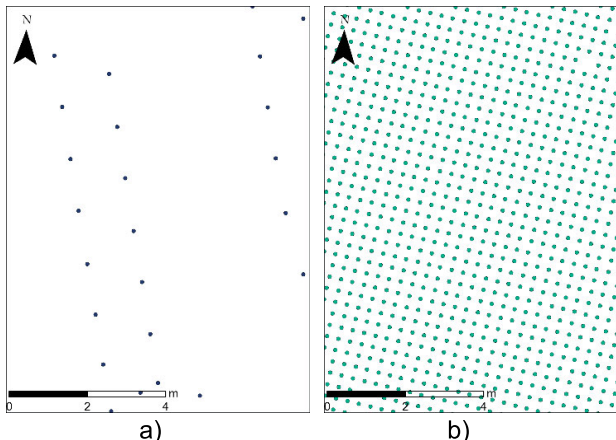


Fig. 1. Comparison of seabed coverage between measurements recorded using: a) singlebeam echosounders (SBES), b) multibeam echosounders (MBES); source: own elaboration

In addition to the ability to provide full seabed coverage, MBES data are characterised by high accuracy and resolution. Measurements performed with these systems also increase the efficiency of survey operations (Grządziel and Wąż, 2016). To ensure the required level of coverage, proper planning of the shape and spacing of survey lines is essential (Specht *et al.*, 2019). The method for calculating this spacing is specified in the EM 1110-2-1003 USACE Standards for Hydrographic Surveys (USACE, 2013):

$$L = 2d \cdot \tan\left(\frac{a}{2}\right) \cdot (1 - s) \quad (1)$$

where: L = distance between sounding profiles, d = depth of the waterbody, a = MBES swath angle, s = overlap zone between neighbouring swaths.

Table 1. Technical specifications of the AutoDron USV

Technical data	AutoDron USV	Photo
Dimensions	110x70x10 cm	
Weight	18 kg	
Operating speed	3 kn	
Max. speed	6 kn	
Operating range	1 km	
Telemetry monitoring	integrated with the RC system	
Operating time	3 h	

Source: own elaboration.

When using an MBES on USV platforms, vessel stability and the precise orientation of the transducer during measurements are critically important. Due to their low displacement and high susceptibility to wave action, USVs require accurate synchronisation of data from GNSS and IMU systems to compensate for platform movements. Careful planning of survey lines and control of vessel speed is essential to ensure the required data quality and continuity, in accordance with IHO guidelines for the most stringent survey orders (Specht, 2024a; Specht, 2024b).

STUDY AREA, EQUIPMENT USED, AND SURVEY PROCEDURE

The bathymetric measurements were conducted on Lake Kłodno, located in Kartuzy County (Pomeranian Voivodship), within the Kashubian Landscape Park. The lake, with a surface area of 134.9 ha and a length of approximately 2 km, reaches a maximum depth of 38.5 m. According to data published by the Chief Inspectorate of Environmental Protection (Pol.: Główny Inspektorat Ochrony Środowiska – GIOŚ) for 2019–2024, Lake Kłodno is classified as having moderate ecological status (Zalewski, 2025). The surveyed area covered the shallow water zone of the lake, with depths ranging from 0.5 to 11.1 m.

Two USV platforms were used in the study: one equipped with an SBES and the other with an MBES. In the shallow part of the waterbody (depths below 1 m), a compact AutoDron USV was used. This small catamaran, measuring 110x70x10 cm and weighing approximately 18 kg (including measurement equipment), was equipped with a SonarMite BTX SBES and a Trimble R10 GNSS RTK receiver, allowing precise determination of measurement point coordinates. The basic technical specifications of the AutoDron USV and the SBES are presented in Tables 1 and 2.

In the deeper part of the lake, the HydroDron-1 USV was used. This catamaran has dimensions of 4x2 m and has a draft of 0.5 m. It was equipped with a PING 3DSS-DX-450 MBES, an SBG Ekinox2-U GNSS/INS system, and a remotely controlled hydrographic head. Additionally, it featured a situational monitoring system comprising a weather station and cameras, enhancing safety and enabling real-time operational control during the survey. The basic technical specifications of the HydroDron-1 USV and the MBES are presented in Tables 3 and 4.

The bathymetric measurements were adapted to the specific characteristics of the USV platforms used and the prevailing hydrometeorological conditions. On 1 August 2023, measure-

Table 2. Technical specifications of the SonarMite BTX SBES

Technical parameter	SonarMite BTX SBES	Photo
Transducer frequency	235 kHz	
Beam spread	4°	
Depth range	0.3–75.0 m	
Depth measurement accuracy	0.025 m RMS	
Sound velocity range	1,400–1,600 m·s ⁻¹	
Data output range	2 Hz	
Ping rate	3–6 Hz	phot.: Geotronics Polska (2025)

Source: own elaboration.

Table 3. Technical specifications of the HydroDron-1 USV

Technical data	HydroDron-1 USV	Photo
Dimensions	4×2×0.5 m	
Weight	300 kg	
Operating speed	3–4 kn	
Max. speed	14 kn	
Operating range	6 km	
Telemetry monitoring	integrated with the RC system	
Operating time	12 h	phot.: O. Specht

Source: own elaboration.

Table 4. Technical specifications of the PING 3DSS-DX-450 MBES

Technical parameter	PING 3DSS-DX-450 MBES	Photo
Operating frequency	450 kHz	
Bathymetry swath width	8–16 times sonar altitude	
Max bathymetry range	100 m per side	
Depth range	0.7–75 m	
Sounding accuracy	exceeds IHO Special Order	
Multibeam mode settings	beamwidth: 0.25–5° sector: 90–220° beams: 3–1,024	
Bin width	5–200 cm	
Max. ping repetition rate	30 Hz	phot.: Geo-matching (2025)

Source: own elaboration.

ments were first conducted using the HydroDron-1 USV. Survey lines followed seven profiles parallel to the shoreline, covering the deeper part of the lake. The arrangement of these profiles ensured complete bottom coverage and sufficient data density in accordance with IHO S-44 requirements.

Subsequently, on 23 August 2023, measurements were carried out using the AutoDron USV. A total of 41 survey profiles were laid out at 10-metre intervals and oriented perpendicular to the shoreline, enabling high-resolution mapping of the shallow water zone. Given depths of less than 1 m, the routes were carefully planned to avoid sensor collisions with the lakebed and underwater obstacles.

Measurements were conducted exclusively under windless conditions, with a sea state of 0–1 on the Douglas scale, to minimise the influence of wave motion and surface currents on the quality of the bathymetric data. The use of two independent USV platforms, each equipped with a different measurement system (SBES and MBES), enabled a comparative analysis of the spatial completeness and uniformity of the data, forming the basis for the subsequent part of the study.

PROCESSING BATHYMETRIC DATA FROM SBES AND MBES

Bathymetric data are assigned coordinates in a flat, rectangular coordinate system based on differential GNSS RTK measurements and depth values recorded by the echo sounder. The first step in processing data obtained from SBES or MBES systems is to reference the depth measurements to the official national vertical datum. In Poland, depths must be reported using the PL-EVRF2007-NH normal height system, where the reference level ($H = 0.000$ m) corresponds to the Amsterdam Ordnance Datum (Fig. 2) (Rozporządzenie, 2012; Rozporządzenie, 2019).

The normal height of a measurement point, referenced to the PL-EVRF2007-NH system, is calculated using the following formula (Lewicka *et al.*, 2022):

$$H_{\text{PL-EVRF2007-NH}} = -(d_e + \Delta d_e \pm \Delta d_{\text{PL-EVRF2007-NH}}) \quad (2)$$

where: $H_{\text{PL-EVRF2007-NH}}$ = normal height of the measurement point, d_e = depth recorded by the echo sounder, Δd_e = draft of the

echo sounder transducer, $\Delta d_{\text{PL-EVRF2007-NH}}$ = depth correction relative to the reference level; if the sea level is <500 cm, the correction should be added; otherwise, it should be subtracted.

The value of the depth correction is determined using the following formula (Lewicka *et al.*, 2022):

$$\Delta d_{\text{PL-EVRF2007-NH}} = 500 \text{ cm} - \bar{d}_{\text{SW}_{\text{PL-EVRF2007-NH}}} \quad (3)$$

where: $\bar{d}_{\text{SW}_{\text{PL-EVRF2007-NH}}}$ = mean sea level recorded by the tide gauge between two consecutive full hours.

The selection of an appropriate hydrometeorological station is crucial, as it should be located as close as possible to the surveyed water body. In the absence of such a station, and under calm wave conditions, it is acceptable to reference depth measurements to the current water surface level, which can be determined, for example, using GNSS RTK measurements taken along the 0 m isobath. Alternatively, remote sensing methods such as light detection and ranging (LiDAR) may be used (Lewicka *et al.*, 2022).

The next stage in processing depth data is data cleaning, which aims to remove outliers and erroneous measurements. For data collected using an SBES, this process primarily involved manually reviewing the survey profiles. Special attention was given to the shallow water zone (depths below 1 m), where measurements are particularly affected by errors caused by wave motion, signal disturbances, and limited platform stability. Points identified as erroneous were removed (Deunf Le *et al.*, 2020).

For data collected using an MBES, a depth filter was applied to exclude observations outside the 2–11 m range. This interval was determined based on an analysis of seabed topography and the equipment's technical specifications. After automatic filtering, a manual data review was carried out to identify and remove measurement errors caused, among other factors, by multiple signal reflections, underwater vegetation, or instability of the USV.

The cleaned and prepared data are ready for further processing and spatial analysis, including the creation of DBMs. Proper vertical referencing, high-quality filtering, and effective noise elimination are crucial for obtaining reliable measurement results and meeting IHO requirements.

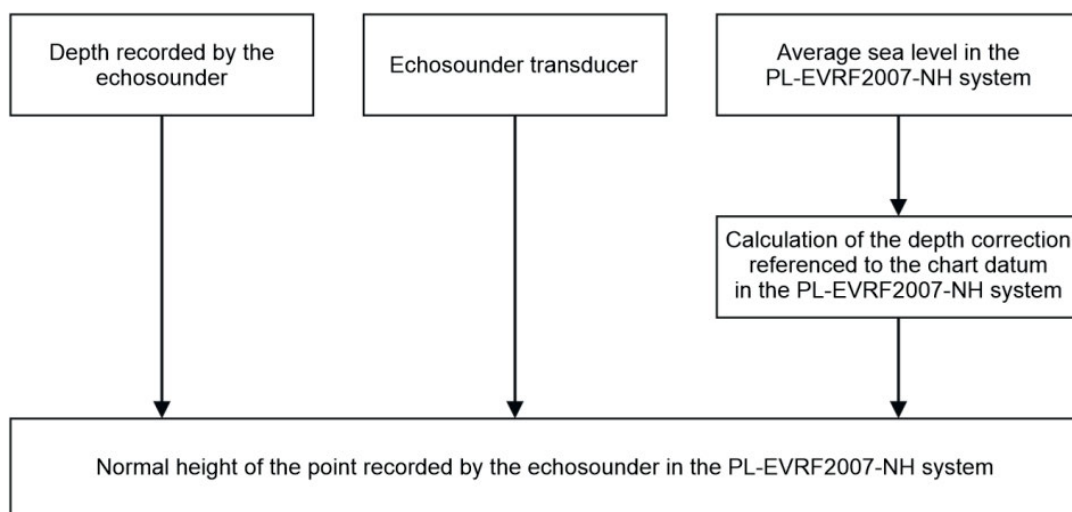


Fig. 2. A flowchart illustrating the steps involved in determining depth relative to a fixed reference level; source: own elaboration

RESULTS AND DISCUSSION

SINGLEBEAM ECHOSOUNDERS RESULTS AND INTERPRETATION

Bathymetric measurements in the shallow water zone of Lake Kłodno were conducted on 23 August 2023 using a SonarMite BTX SBES integrated with a Trimble R10 GNSS RTK receiver. The measurement setup enabled the recording of depth data at a frequency of 1 Hz. A total of 7,006 points were collected during the survey, with an average accuracy of 0.05 m in the horizontal plane and 0.06 m in the vertical plane. After manual data cleaning, the number of points was reduced by 17%. Most of the erroneously recorded data occurred near the shoreline (Fig. 3).

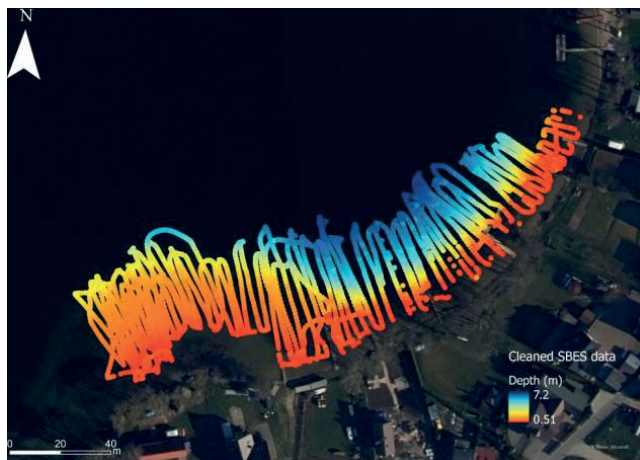


Fig. 3. Cleaned singlebeam echosounders (SBES) data for Lake Kłodno; source: own study

Bathymetric measurements in the shallow water zone of Lake Kłodno were conducted on 23 August 2023 using a SonarMite BTX SBES integrated with a Trimble R10 GNSS RTK receiver. The measurement setup enabled the recording of depth data at a frequency of 1 Hz. A total of 7,006 points were collected during the survey, with an average accuracy of 0.05 m in the horizontal plane and 0.06 m in the vertical plane. After manual data cleaning, the number of points was reduced by 17%. Most of the erroneously recorded data occurred near the shoreline (Fig. 3).

Data of SBES primarily cover the nearshore zone of the lake. Measurement points are unevenly distributed due to the survey method employed. The colour scale shows a gradual increase in depth, from approximately 0.5 m near the shoreline to over 7 m in the central part of the lake. In some areas, clusters of measurement points are visible, likely resulting from frequent turns or temporary stops of the USV.

To assess the distribution of SBES data, a regular 1×1 m grid was created as the basis for further spatial analysis. Based on the cleaned bathymetric data, the grid was generated and clipped to the actual extent of the measurement points. This enabled clear identification of cells that contain data and those that remain empty. The grid facilitated the detection of surveyed areas and the identification of data gaps, providing a solid foundation for evaluating the quality and completeness of the lake's bathymetric coverage (Fig. 4).

The data gaps visible in Figure 4 are primarily located in the nearshore zone of the lake. These result from equipment

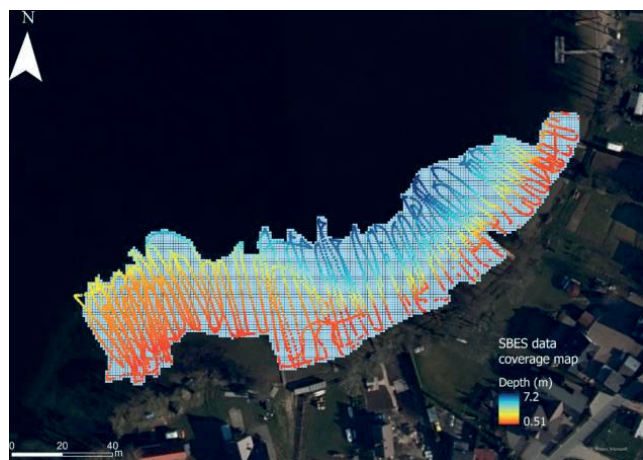


Fig. 4. Singlebeam echosounders (SBES) data coverage map in a 1×1 m grid for Lake Kłodno; source: own study

limitations that prevent effective bathymetric measurements in very shallow inland waters, particularly in the area between the 0 and 0.5 m isobaths. Additionally, data collection in these areas was hindered by physical obstacles such as dense shoreline vegetation, floating docks, and moored vessels located both near the docks and at various points along the shoreline. These features physically restricted the manoeuvrability of the USV, making it difficult to conduct measurements near the shore.

Larger distances between survey profiles, observed in the central part of the lake, may be attributed to the limited positioning accuracy of the USV (Global Positioning System (GPS) + Russian Global Navigation Satellite System (Rus. Global'naya navigatsionnaya sputnikovaya sistema – GLONASS)) and the method used to conduct the survey, whether automatic or manual. Depending on local conditions, the control mode, and the quality of the GNSS signal, the spacing between successive profiles could vary, contributing to uneven spatial coverage.

Next, point density classification was conducted for the cells of the grid, based on NOAA guidelines recommending a minimum data density of $5 \text{ pts} \cdot \text{m}^{-2}$ (Office of Coast Survey, 2021). Four classes were defined: no data (0 pts), low density (1–4 pts), medium density (5–9 pts), and very high density (≥ 10 pts). Detailed class ranges and their descriptions are provided in Table 5.

The spatial distribution of SBES data density classes for Lake Kłodno is presented in Figure 5. The applied colour scale enables the identification of areas with varying degrees of bathymetric coverage.

In Figure 5, red indicates 5,366 grid cells (63.79%) without data, located primarily in the nearshore zone and in areas where survey profiles are discontinuous. Grid cells with low point density ($1\text{--}4 \text{ pts} \cdot \text{m}^{-2}$), marked in yellow, account for 2,895 cells (34.42%) and dominate the analysed area. This reflects the presence of data, although the density does not reach the level recommended by NOAA guidelines. Areas that meet the minimum NOAA requirement ($\geq 5 \text{ pts} \cdot \text{m}^{-2}$), marked in light and dark blue, comprise a total of 151 grid cells (1.79%). These are scattered and occur mainly where USV routes overlapped or where the vessel temporarily stopped. The spatial distribution of density classes indicates that a significant part of the lake was surveyed at low point density, which may affect the accuracy of the resulting bathymetric model and shows the need to supplement data in selected areas.

Table 5. Classification of bathymetric data density in a 1×1 m grid

Class	Number of points ($\text{pts} \cdot \text{m}^{-2}$)	Description of data density
None	0	no data – empty grid cells
Low	1–4	low density – below NOAA recommendations
Medium	5–9	meets minimum requirements ($\geq 5 \text{ pts} \cdot \text{m}^{-2}$ in accordance with NOAA guidelines)
Very high	≥ 10	high density – highly detailed data

Source: own study.



Fig. 5. Singlebeam echosounders (SBES) data density categorisation in a 1×1 m grid for Lake Kłodno; source: own study

To compare data acquired using MBES and SBES echo sounders, statistical measures of point density within the grid cells were analysed. The R68 and R95 measures, calculated by sorting values in descending order, were used as criteria for evaluating depth data density. The R68 represents the minimum number of points exceeded by 68% of the grid cells, while the R95 indicates the value exceeded by 95% of cells. These measures are advantageous because they do not rely on assumptions about the underlying statistical distribution and provide a high level of confidence. Additionally, standard statistical measures such as the

arithmetic mean, standard deviation, and minimum and maximum values were calculated.

The average number of points per individual grid cell was 0.69, with a standard deviation of 3.11. Point counts per cell ranged from 0 to 197. This wide variation resulted from the specifics of the survey process, as the highest point densities were recorded at the beginning and end of survey profiles, where the USV slowed down or temporarily stopped. The R68 and R95 values were 2 points and 1 point, respectively, indicating that a significant part of the surveyed area was characterised by a very low number of recorded points. The distribution of points across grid cells is shown in the histogram (Fig. 6), which provides insight into data dispersion.

MULTIBEAM ECHOSOUNDERS RESULTS AND INTERPRETATION

Bathymetric measurements in the deep-water area of Lake Kłodno were conducted on 1 August 2023 using a PING 3DSS-DX-450 MBES. The device emits acoustic pulses via 512 separate beams at a frequency of 100 Hz, enabling the rapid acquisition of a dense point cloud representing the lakebed topography. Initial data processing included removing points outside the 2–11 m depth range, as well as manually cleaning erroneous values (Fig. 7).

Based on Figure 7, it can be concluded that the MBES data covers the deep-water part of Lake Kłodno, excluding the nearshore zone, which was too shallow for the HydroDron-1 USV. The colour scale shows a systematic increase in depth

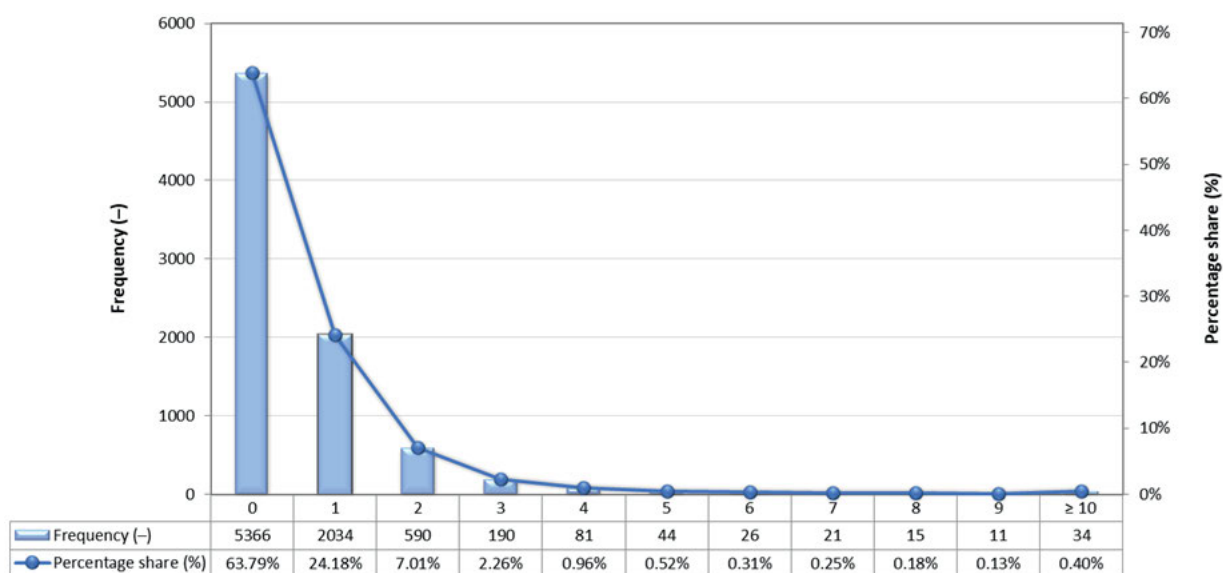


Fig. 6. Histogram of the number of singlebeam echosounders (SBES) points per grid cell for Lake Kłodno; source: own study

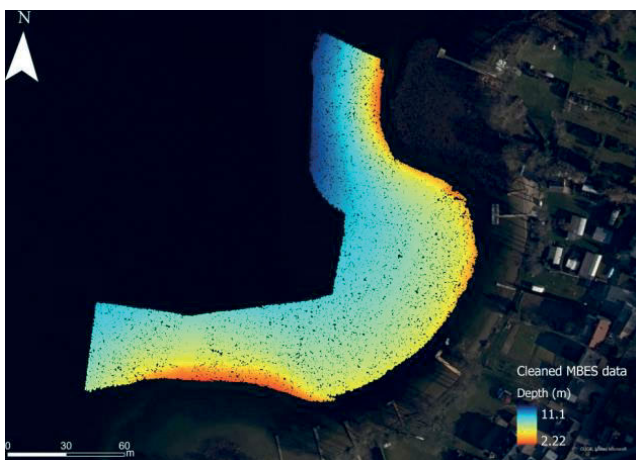


Fig. 7. Cleaned multibeam echosounders (MBES) data for Lake Kłodno: source: own study

toward the centre of the lake, starting at approximately 2.2 m near the shore and reaching over 11 m in the deepest areas. The measurement points are densely and evenly distributed, indicating high-quality data acquisition. Measurements of SBES supplement the MBES data in the nearshore zone, which was inaccessible to the interferometric echo sounder.

To evaluate the distribution of MBES data in the deep-water area of Lake Kłodno, a 1×1 m resolution grid was created. The analysis enabled the assessment of spatial coverage and the identification of areas with no measurements. The results are presented as a data coverage map (Fig. 8) and a point density categorisation map (Fig. 9).

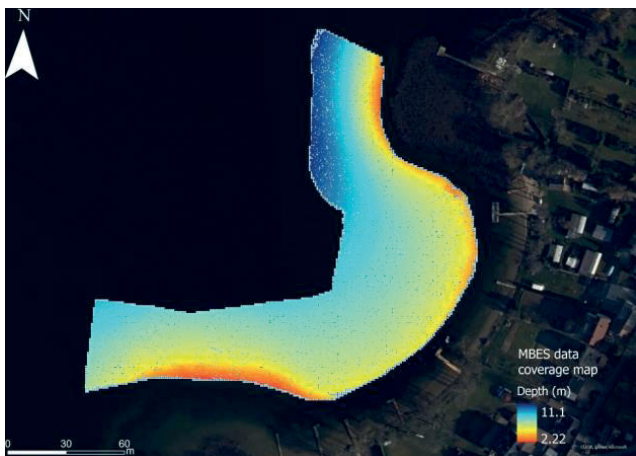


Fig. 8. Multibeam echosounders (MBES) data coverage map in a 1×1 m grid for Lake Kłodno; source: own study

In Figure 9, red indicates 424 grid cells (2.88%) with no data, located primarily at the edges of the echo sounder's operational range. Cells with sparse point density ($1-4 \text{ pts} \cdot \text{m}^{-2}$), marked in yellow, account for 416 cells (2.83%) and are distributed sporadically. This suggests the presence of data, although the density does not meet the minimum standards specified in NOAA guidelines. Areas that meet these standards ($\geq 5 \text{ pts} \cdot \text{m}^{-2}$), shown in light blue and dark blue, comprise 13,864 grid cells (94.29%) and dominate the surveyed area. The spatial distribution of density classes indicates that nearly the entire survey area is covered by high-density, uniformly distributed data, enabling the development of a detailed, high-resolution bathymetric model.



Fig. 9. Multibeam echosounders (MBES) data density categorisation in a 1×1 m grid for Lake Kłodno: source: own study

Based on the cleaned MBES data, a 1-metre resolution grid was generated. Statistical analysis showed that each square metre contained an average of 7.71 pts, with a standard deviation of 1.82. The number of points per cell ranged from 0 to 10, and the R68 and R95 values were 9 and 8 pts, respectively. These results confirm that the MBES data exhibit high and uniform spatial density throughout the analysed area (Fig. 10).

In summary, MBES provided significantly greater data density and uniformity than SBES. While SBES enabled measurements in areas inaccessible to MBES, its point distribution was irregular and sparse. The combined use of both measurement technologies, which complement each other in terms of coverage and data density, enables the creation of a detailed and coherent bathymetric model of Lake Kłodno.

COMPARATIVE DISCUSSION AND IMPLICATIONS

The analysis of bathymetric data collected using the SBES and MBES systems, mounted on separate USV platforms, revealed significant differences in the quality, density, and spatial distribution of the measurement points. Both technologies offer advantages but also have limitations arising from equipment design and the hydrographic conditions of the surveyed waterbody. Table 6 presents a comparison of key parameters for SBES and MBES.

The SBES system proved effective in recording data in the shallow coastal zone of Lake Kłodno, where the use of MBES was impossible due to limited depth and the presence of obstacles such as shoreline vegetation, piers, and moored vessels. Despite this functionality, SBES data were characterised by low and uneven density. Only 1.79% of grid cells contained data meeting the minimum NOAA requirements (at least $5 \text{ pts} \cdot \text{m}^{-2}$), while 63.79% of cells contained no measurement points.

Data obtained from the MBES system was characterised by significantly higher spatial density and uniform distribution of points. Over 94% of the grid cells contained data exceeding the minimum value recommended by NOAA, with an average point density of $7.71 \text{ pts} \cdot \text{m}^{-2}$ and a standard deviation of $1.82 \text{ pts} \cdot \text{m}^{-2}$. This distribution indicates very high quality and completeness of coverage, enabling the development of a detailed, high-resolution bathymetric model. The high density and homogeneity of MBES data not only allow for the creation of accurate bathymetric

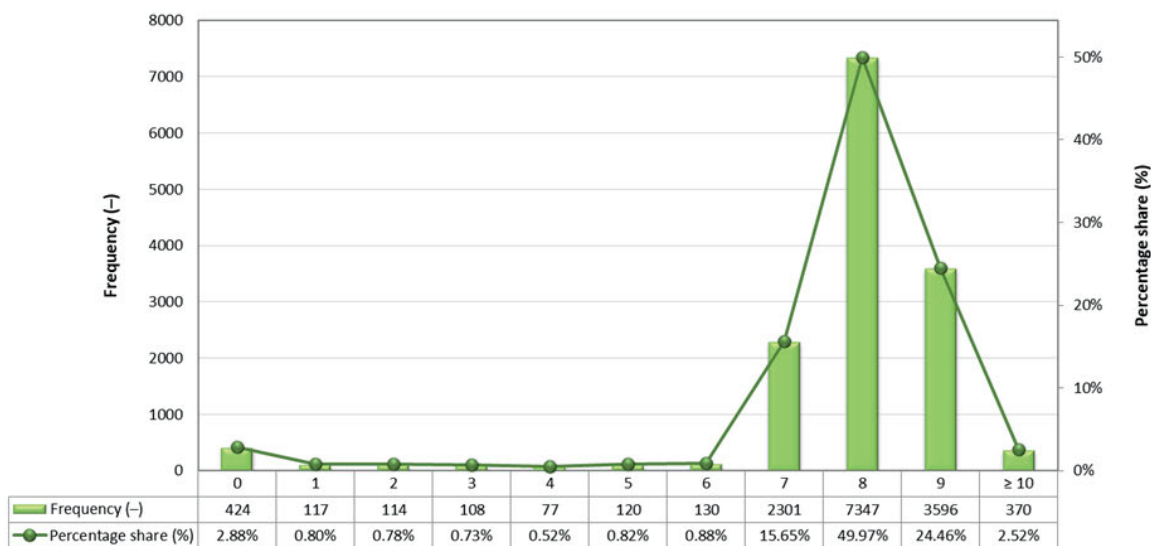


Fig. 10. Histogram of the number of multibeam echosounders (MBES) points per grid cell for Lake Kłodno; source: own study

Table 6. Comparison of selected measurement parameters of the singlebeam echosounders (SBES) and multibeam echosounders (MBES) systems

Parameter	SBES	MBES
Number of grid cells	8,412	14,704
Depth range	0.51–7.20 m	2.22–11.10 m
Average point density	0.69 pts·m ⁻²	7.71 pts·m ⁻²
Standard deviation of point density	3.11 pts	1.82 pts
Range of points per grid cell	0–197 pts	0–10 pts
R68/R95 measure	2 pts / 1 pt	9 pts / 8 pts
No data (0 pts)	5,366 cells (63.79%)	424 cells (2.88%)
Sparse density (1–4 pts·m ⁻²)	2,895 cells (34.42%)	416 cells (2.83%)
Coverage of cells ≥ 5 pts·m ⁻²	151 cells (1.79%)	13,864 cells (94.29%)

Source: own study.

models but also support activities related to hydrotechnical infrastructure planning, sediment monitoring, and navigation safety.

The comparison showed that MBES significantly outperforms SBES in terms of coverage completeness and quality. However, optimal results are achieved through the proper combination of both technologies, tailored to local hydrographic conditions. The obtained results are consistent with those presented by Mohammadivojdan *et al.* (2025) and in the Hydrographic Survey Specifications and Deliverables report (Office of Coast Survey, 2021), which confirmed homogeneous coverage and data density exceeding 5 pts·m⁻² for MBES. Moreover, the obtained SBES data density (below 1 pts·m⁻²) and its distribution are similar to the results presented by Lubczonk *et al.* (2022).

This summary shows that the effectiveness of bathymetric measurements depends on selecting the appropriate technology based on local depth and environmental conditions. Integrating

SBES and MBES data enables the acquisition of bathymetric data with the highest completeness, which is essential for developing reliable and detailed seafloor models.

CONCLUSIONS

Singlebeam echosounders (SBES) are primarily used in shallow waters, particularly in coastal zones, where other technologies may be less effective due to very low depths and terrain obstacles. However, its limited data density and irregular distribution often require complementary sources to improve bathymetric model quality and to meet standards such as the NOAA-recommended minimum of 5 pts·m⁻².

In very shallow areas, SfM photogrammetry based on unmanned aerial vehicle (UAV) imagery is particularly valuable, as it enables the creation of dense point clouds in locations where hydroacoustic systems provide limited coverage. The choice between structure from motion (SfM) and bathymetric light detection and ranging (LiDAR) should depend on local environmental conditions and water clarity.

Multibeam echosounders (MBES) provide high-density, uniformly distributed data, ensuring reliable bathymetric models. In the analysed case, more than 94% of 1×1 m grid cells exceeded the 5 pts·m⁻² threshold, allowing detailed and accurate seafloor representation. Despite challenges in very shallow waters due to collision risks, MBES clearly outperformed SBES in point count, density, and distribution uniformity.

The both echosounders complement each other, and with proper survey planning and adaptation to local hydrographic conditions, high efficiency and completeness can be achieved. Further work should focus on supplementing shallow-water data using bathymetric LiDAR, global navigation satellite system real time kinematic (GNSS RTK) surveys, or SfM photogrammetry. Future studies should also evaluate whether the resulting models comply with standards of International Hydrographic Organization for the most stringent hydrographic survey orders. Ultimately, only an integrated approach that combines multiple measurement technologies can ensure reliable and comprehensive bathymetric models.

ABBREVIATIONS

a = MBES swath angle
 ALB = airborne lidar bathymetry
 d = depth of the waterbody
 DBM = digital bathymetric model
 d_e = depth recorded by the echo sounder
 GIOŚ = Chief Inspectorate of Environmental Protection (Pol.: Główny Inspektorat Ochrony Środowiska)
 GIS = geographic information system
 GLONASS = Russian Global Navigation Satellite System (Rus.: Global'naya navigatsionnaya sputnikovaya sistema)
 GNSS = Global Navigation Satellite System
 GPS = Global Positioning System
 GUM = Guide to the Expression of Uncertainty in Measurement
 $H_{PL-EVRF2007-NH}$ = normal height of the measurement point
 IDW = inverse distance weighting
 IHO = International Hydrographic Organization
 IMU = inertial measurement unit
 INS = inertial navigation system
 L = distance between sounding profiles
 LiDAR = light detection and ranging
 MBA = multilevel B-spline approximation
 MBES = multibeam echosounder
 MRU = motion reference unit
 NOAA = National Oceanic and Atmospheric Administration
 RTK = real time kinematic
 s = overlap zone between neighbouring swaths
 SBES = singlebeam echosounder
 SDB = satellite-derived bathymetry
 SfM = structure from motion
 SVS = sound velocity sensor
 t = timestamp
 USV = unmanned surface vehicle
 X = northing coordinate
 Y = easting coordinate
 Δd_e = draft of the echo sounder transducer
 $\Delta d_{PL-EVRF2007-NH}$ = depth correction relative to the reference level
 $\bar{d}_{SW_{PL-EVRF2007-NH}}$ = mean sea level recorded by the tide gauge between two consecutive full hours

FUNDING

This research was funded from the statutory activities of Gdynia Maritime University, grant number WN/2026/PZ/05.

CONFLICT OF INTERESTS

The author declares no conflicts of interest.

REFERENCES

Apollo, M. *et al.* (2023) "Geodata in science – A review of selected scientific fields," *Acta Scientiarum Polonorum Formatio Circumiectus*, 22, pp. 17–40. Available at: <https://doi.org/10.15576/ASP.FC/2023.22.2.02>.

Arseni, M. *et al.* (2019) "Testing different interpolation methods based on single beam echosounder river surveying: Case study Siret River," *ISPRS International Journal of Geo-Information*, 8, 507. Available at: <https://doi.org/10.3390/ijgi8110507>.

Bentivoglio, R. *et al.* (2022) "Deep learning methods for flood mapping: A review of existing applications and future research directions," *Hydrology and Earth System Sciences*, 26, pp. 4345–4378. Available at: <https://doi.org/10.5194/hess-26-4345-2022>.

Bodus-Olkowska, O. and Włodarczyk-Sielicka, M. (2013) "Analiza porównawcza i interpretacyjna uogólnionej wizualizacji widoku podwodnego uzyskanego za pomocą echosondy jedno- i wielowiązkowej [Comparative and interpretative analysis of generalised visualisation of the underwater view obtained using single-beam and multibeam echosounders]," *Roczniki Geomatyki*, 11, pp. 27–36.

David, C.G. *et al.* (2021) "Structure-from-motion on shallow reefs and beaches: Potential and limitations of consumer-grade drones to reconstruct topography and bathymetry," *Coral Reefs*, 40, pp. 835–851. Available at: <https://doi.org/10.1007/s00338-021-02088-9>.

Deunf Le, J. *et al.* (2020) "A review of data cleaning approaches in a hydrographic framework with a focus on bathymetric multi-beam echosounder datasets," *Geosciences*, 10, 254. Available at: <https://doi.org/10.3390/geosciences10070254>.

Fernández-Nóvoa, D., González-Cao, J. and García-Feal, O. (2024) "Enhancing flood risk management: A comprehensive review on flood early warning systems with emphasis on numerical modeling," *Water*, 16, 1408. Available at: <https://doi.org/10.3390/w16101408>.

Gao, J. (2009) "Bathymetric mapping by means of remote sensing: Methods, accuracy and limitations," *Progress in Physical Geography*, 33, pp. 103–116. Available at: <https://doi.org/10.1177/030913309105657>.

Geo-matching (2025) 3DSS-DX. Available at: <https://geo-matching.com/products/3dss-dx> (Accessed: August 4, 2025).

Geotronics Polska (2025) Ohmex SonarMite. Available at: <https://geotronics.com.pl/produkty-i-rozwiazania/pomiary-hydrograficzne/ohmex-sonarmite/> (Accessed: August 4, 2025).

Grządziel, A. (2022) "Application of remote sensing techniques to identification of underwater airplane wreck in shallow water environment: Case study of the Baltic Sea, Poland," *Remote Sensing*, 14, 5195. Available at: <https://doi.org/10.3390/rs14205195>.

Grządziel, A. and Wąż, M. (2016) "Estimation of effective swath width for dual-head MBES," *Annual of Navigation*, 23, pp. 173–183. Available at: <https://doi.org/10.1515/aon-2016-0012>.

Haris, K. *et al.* (2012) "Seabed habitat mapping employing single and multi-beam backscatter data: A case study from the western continental shelf of India," *Continental Shelf Research*, 48, pp. 40–49. Available at: <https://doi.org/10.1016/j.csr.2012.08.010>.

IHO (2005) *Manual on hydrography. Publication C-13*. 1st edn. Monaco: International Hydrographic Organization. Available at: https://ihodata.int/uploads/user/pubs/cb/c-13/english/C-13_Chapter_1_and_contents.pdf (Accessed: January 22, 2026).

IHO (2022) *IHO standards for hydrographic surveys*. S-44. 6.1.0 edn. Monaco: International Hydrographic Organization. Available at: https://ihodata.int/uploads/user/pubs/standards/s-44/S-44_Edition_6.1.0.pdf (Accessed: January 22, 2026).

Jung, J. *et al.* (2022) "Multi-modal sonar mapping of offshore cable lines with an autonomous surface vehicle," *Journal of Marine Science and Engineering*, 10, 361. Available at: <https://doi.org/10.3390/jmse10030361>.

Khomsin, Pratomo, D.G. and Saputro, I. (2021) "Comparative analysis of singlebeam and multibeam echosounder bathymetric data,"

IOP Conference Series: Materials Science and Engineering, 1052, 012015. Available at: <https://doi.org/10.1088/1757-899X/1052/1/012015>.

Landero Figueroa, M.M. et al. (2021) "The use of singlebeam echosounder depth data to produce demersal fish distribution models that are comparable to models produced using multibeam echosounder depth," *Ecology and Evolution*, 11, pp. 17873–17884. Available at: <https://doi.org/10.1002/ece3.8351>.

Lewicka, O. et al. (2022) "Analysis of transformation methods of hydroacoustic and optoelectronic data based on the tombolo measurement campaign in Sopot," *Remote Sensing*, 14, 3525. Available at: <https://doi.org/10.3390/rs14153525>.

Li, Z. et al. (2023) "Exploring modern bathymetry: A comprehensive review of data acquisition devices, model accuracy, and interpolation techniques for enhanced underwater mapping," *Frontiers in Marine Science*, 10, 1178845. Available at: <https://doi.org/10.3389/fmars.2023.1178845>.

Lubczonek, J. et al. (2022) "Methodology for combining data acquired by unmanned surface and aerial vehicles to create digital bathymetric models in shallow and ultra-shallow waters," *Remote Sensing*, 14, 105. Available at: <https://doi.org/10.3390/rs14010105>.

Lubis, M.Z. et al. (2019) "Review: Bathymetry mapping using underwater acoustic technology," *Journal of Geoscience, Engineering, Environment, and Technology*, 4, pp. 135–138. Available at: <https://doi.org/10.25299/jgeet.2019.4.2.3127>.

Makar, A. (2023) "Coastal bathymetric sounding in very shallow water using USV: Study of public beach in Gdynia, Poland," *Sensors*, 23, 4215. Available at: <https://doi.org/10.3390/s23094215>.

Mitchell, N.C. and Hughes Clarke, J.E. (1994) "Classification of seafloor geology using multibeam sonar data from the Scotian Shelf," *Marine Geology*, 121, pp. 143–160. Available at: [https://doi.org/10.1016/0025-3227\(94\)90027-2](https://doi.org/10.1016/0025-3227(94)90027-2).

Mohammadirojdan, B. et al. (2025) "Enhancing digital bathymetric models by advanced measurement uncertainty analysis," *International Hydrographic Review*, 31, pp. 28–50

NORBIT (2022) *Wideband multibeam sonar*. Available at: <https://www.uniquegroup.com/wp-content/uploads/2022/08/WBMS-data-sheet.pdf> (Accessed: August 4, 2025).

Office of Coast Survey (2021) *Hydrographic survey specifications and deliverables*. Office of Coast Survey NOAA. Available at: https://nauticalcharts.noaa.gov/publications/docs/standards-and-requirements/specs/HSSD_2021.pdf (Accessed: August 4, 2025).

Orange, D.L. et al. (2002) "Tracking California seafloor seeps with bathymetry, backscatter and ROVs," *Continental Shelf Research*, 22, pp. 2273–2290. Available at: [https://doi.org/10.1016/S0278-4343\(02\)00054-7](https://doi.org/10.1016/S0278-4343(02)00054-7).

Popielarczyk, D. (2011) "Application of global navigation satellite system and hydroacoustic techniques to safety of inland water navigation," *Archives of Transport*, 23, pp. 191–207. Available at: <https://doi.org/10.2478/v10174-011-0013-x>.

Purnawan, S. et al. (2025) "Seabed classification of coral reef environments using 200 kHz single-beam echosounder and machine learning techniques," *Egyptian Journal of Aquatic Research*, 51, pp. 341–351. Available at: <https://doi.org/10.1016/j.ejar.2025.06.001>.

Rozporządzenie (2012) "Rozporządzenie Rady Ministrów z dnia 15 października 2012 r. w sprawie państwowego systemu odniesień przestrzennych [Regulation of the Council of Ministers of 15 October 2012 on the national spatial reference system]," *Dz.U.* 2012 poz. 1247.

Rozporządzenie (2019) "Rozporządzenie Rady Ministrów z dnia 19 grudnia 2019 r. zmieniające rozporządzenie w sprawie państwowego systemu odniesień przestrzennych [Regulation of the Council of Ministers of 19 December 2019 amending the regulation on the national spatial reference system]," *Dz.U.* 2019 poz. 2494.

Salamon, R. (2006) *Systemy hydrolokacyjne [Hydroacoustic systems]*. Gdańsk: Gdańskie Towarzystwo Naukowe.

Specht, C., Specht, M. and Dabrowski, P. (2017) "Comparative analysis of active geodetic networks in Poland," in *Proceedings of the 17th International Multidisciplinary Scientific GeoConference (SGEM 2017)*, 17(22), Jun 27–Jul 6, 2017, Albena, Bulgaria. Sofia: SGEM, pp. 163–176.

Specht, M. (2024a) "Methodology for performing bathymetric and photogrammetric measurements using UAV and USV vehicles in the coastal zone," *Remote Sensing*, 16, 3328. Available at: <https://doi.org/10.3390/rs16173328>.

Specht, M. (2024b) "Testing and analysis of selected navigation parameters of the GNSS/INS system for USV path localization during inland hydrographic surveys," *Sensors*, 24, 2418.

Specht, M. et al. (2019) "Methodology for performing territorial sea baseline measurements in selected waterbodies of Poland," *Applied Sciences*, 9, 3053. Available at: <https://doi.org/10.3390/s24082418>.

Specht, M. et al. (2020) "The use of USV to develop navigational and bathymetric charts of yacht ports on the example of National Sailing Centre in Gdańsk," *Remote Sensing*, 12, 2585. Available at: <https://doi.org/10.3390/rs12162585>.

Specht, O. (2023) "Multi-sensor integration of hydroacoustic and optoelectronic data acquired from UAV and USV vehicles on the inland waterbody," *TransNav: International Journal on Marine Navigation and Safety of Sea Transportation*, 17, pp. 791–798. Available at: <https://dx.doi.org/10.12716/1001.17.04.04>.

Stateczny, A., Gronska-Sledz, D. and Motyl, W. (2019) "Precise bathymetry as a step towards producing bathymetric electronic navigational charts for comparative (terrain reference) navigation," *Journal of Navigation*, 72, pp. 1623–1632. Available at: <https://doi.org/10.1017/S0373463319000377>.

Todd, B.J. et al. (1999) "Quaternary geology and surficial sediment processes, Browns Bank, Scotian Shelf, based on multibeam bathymetry," *Marine Geology*, 161, pp. 165–214.

Trzcinska, K. et al. (2020) "Spectral features of dual-frequency multibeam echosounder data for benthic habitat mapping," *Marine Geology*, 427, 106239. Available at: <https://doi.org/10.1016/j.margeo.2020.106239>.

Tuno, N. et al. (2024) "Analyzing depth uncertainty of near-shore bathymetric survey conducted by single-beam echo sounder," *Tehnički Glasnik*, 18, pp. 84–91. Available at: <https://doi.org/10.31803/tg-20241008141610>.

USACE (2013) *EM 1110-2-1003 USACE standards for hydrographic surveys*. Washington, DC: Department of the Army U.S. Army Corps of Engineers.

Zalewski, T. (2025) *Ocena stanu wód powierzchniowych na podstawie danych z lat 2019–2024. Tabela z wynikami oceny i klasyfikacji jezior* [Assessment of surface water status based on data from 2019–2024. Table with results of lake assessment and classification]. Portal jakości wód powierzchniowych. Warszawa: GIOŚ. Available at: <https://wody.gios.gov.pl/pjwp/publication/568> (Accessed: January, 21, 2026).